Available online at www.dergipark.org.tr/en

INTERNATIONAL ADVANCED RESEARCHES and ENGINEERING JOURNAL

Journal homepage: www.dergipark.org.tr/en/pub/iarej

e-ISSN: 2618-575X

International Open Access

Volume 04
Issue 01

April, 2020

Research Article

Estimation of PM_{10} concentrations in Turkey based on Bayesian maximum entropy

Özlem Baydaroğlu Yeşilköy [a,*]

[a]Altınbaş University, School of Engineering and Natural Sciences, Department of Civil Engineering, İstanbul/Turkey

ARTICLE INFO

Article history:
Received 09 January 2020
Revised 19 February 2020
Accepted 26 February 2020

Keywords:
Air pollution
Bayesian maximum entropy
PM_{10}
Prediction
Spatiotemporal mapping

ABSTRACT

Spatial and temporal distribution of PM_{10} is modeled by Bayesian Maximum Entropy (BME) method. It is the spatiotemporal estimation method which combines exact measurements with the secondary information by considering local uncertainties. In this study, daily average PM_{10} data are used to generate spatial and temporal PM_{10} maps. Both annual and seasonal estimations have been realized. This is the first study which concentrates on spatiotemporal distribution of PM_{10} for all regions of Turkey by using Bayesian Maximum Entropy method. Error variances are used as performance criteria in both seasonal and annual predictions. All prediction results stay within the limits of the confidence intervals. In addition, unknown PM_{10} values are estimated, including PM_{10} values over the seas. It is thought that the PM_{10} maps which show all regions of Turkey in detail are quite invaluable and informative.

1. Introduction

As a mixture of solid and liquid particles, particulate matter (PM) may be originated from natural sources such as windblown dust, anthropogenic sources like agricultural and industrial activities, fossil fuel combustion. Since PMs are of vital significance in respect to air quality phenomenon, estimation and forecast of it enables decision-makers to take precautions.

Bayesian Maximum Entropy (BME) [1, 2, 3, 4, 5, 6] is a nonlinear geostatistical approach. In this method, Bayesian conditionalization and entropy maximization are combined to generate spatiotemporal mapping. When compared to other methods, it is seen that the confidence levels provided by BME are narrow. Moreover, error variances are used as performance criteria of results [7].

BME is the only approach which uses not only raw data but also auxiliary data (soft data) in a spatiotemporal mapping. In other words, different kinds of information are merged [8]. BME realizes gaining, interpreting and processing of information in three stages.

BME is employed for estimation and prediction of different kinds of variables, such as ozone [9], soil moisture [10], rainfall [11], soil salinity [12], sea surface temperature [13] and wind [14].

Although distribution of PM is valuable individually for air quality management purposes, it is also associated with climatological conditions, agricultural activities, industries, residential heating types, topographical features and populations. There are many PM studies in Turkey. Some inventory and estimation studies of PM_{10} can be seen below. Alyuz and Alp [15] prepared an emission inventory of primary air pollutants for Turkey investigating in 7 main categories and 53 sub-sectors. It was stated that the calculated PM emission value for the year 2010 was 48.853 t and PM emissions were mainly emitted from the mineral, metallurgical, pulp and paper industries. Furthermore, Saharan dust was the most significant source of PM in Turkey [16]. Güler ve İşçi [17] used a Fuzzy C-Auto Regressive Model (FCARM) and Autoregressive Model (AR) to reflect the regional behavior of weekly PM_{10} concentrations. Results showed that the former model provided better prediction accuracy. Ozel ve Cakmakyapan [18] developed a new approach which was based on gamma-Poisson process in

* Corresponding author. Tel.: +90-212-6040100
E-mail addresses: ozlembaydaroglu@gmail.com *(Ö. Baydaroğlu Yeşilköy)*
ORCID: 0000-0003-2184-5785 *(Ö. Baydaroğlu Yeşilköy)*
DOI: 10.35860/iarej.672520

order to predict PM_{10} concentrations in Central Anatolia Region by using PM_{10} data from 24 air quality monitoring stations for the years between 2007 and 2013. In this study, daily average PM_{10} concentration was found as 148 $\mu g/m^3$. Im et al. [19] investigated high winter-time PM_{10} values using a high resolution the WRF/CMAQ (Weather and Forecasting Model/Community Modelling Air Quality Model) mesoscale model system. Calculated PM_{10} levels by the model underestimated the observations with an average of 10% at the sampling station. Şahin et al. [20] proposed the cellular neural network (CNN) method in order to modeling air pollutants such as PM_{10} concentrations in İstanbul. Meteorological parameters were used for model inputs. Results of the CNN were compared to statistical persistence method (PER) results and it was seen that the CNN and PER outputs were correlated with observations via statistical performance indices. Results indicated that the CNN was more accurate than the PER. Karaca [21] developed a classification method in order to categorize air zones. Geographic Information System (GIS)-based interpolation method and statistical analysis were used in order to generate PM_{10} pollution profiles for Turkey.

There are also many international studies about modeling, analyzing and forecasting of PM_{10} values in the literature. For instance, chemistry-transport models (CTMs) [22, 23], ensemble models with bias-correction techniques [24] and with machine learning algorithms [25], stepwise regression and wavelet analysis [26], universal kriging, land use regression method [27] were implemented in order to forecast PM_{10} levels. Other studies which used BME in prediction are given below. Christakos and Serre [28] analyzed PM distributions in North Carolina by the BME mapping method. Because one of the most significant phenomena was assessing the uncertainty for each of space/time pollution maps in a stochastic pollutant analysis, standard deviations of BME errors were used as a measure of uncertainty. Besides, standard deviations were zero at monitoring stations while they took higher values at regions away from these stations [28]. Results of the study indicated that the PM_{10} maps showed clear variability. Another PM study was realized by Christakos and Serre [29]. They modeled space/time distribution of PM_{10} for a six-year period and optimized its monitoring network for Thailand. In the north of the city, there was a district seasonal fluctuation of PM_{10} values between December and February where this kind of fluctuation in the South Thailand was not seen. Residential exposure of ambient ozone and PM_{10} values were estimated using BME method at multiple time scales by Yu et al. [30]. The same study was carried out with simple kriging and all results were compared. According to results, the usage of soft data enhanced the accuracy of the forecast. Fernando et al. [31] used a stochastic NN model based on neural network called EnviNNet and CMAQ to predict PM in Phoenix. It was found that EnviNNet predicted PM_{10} concentrations better than the CMAQ. Akita et al. [32] proposed a moving window-BME (MWBME) method in order to forecast $PM_{2.5}$ concentrations. In the study, the results were compared to the stationary kriging (SK) and moving window kriging (MWK). It was seen that MWBME had a good capability to catch the highest correlation between observations and forecast results. $PM_{2.5}$ values in United States were estimated using a Land Use Regression Model (LUR) and BME by Beckerman et al. [33] and it was seen that the hybrid model gave more accurate results than each of other models.

In this study, daily average PM_{10} data from 145 air quality monitoring stations of Ministry of Environment and Urbanization of Turkey have been used. Either annual or seasonal estimations have been realized. Zero and constant-local mean (simple and ordinary kriging) are chosen in the last stage of BME.

In all estimations, Bayesian Maximum Entropy Graphical Users Interface (BMEGUI) has been used [see 34].

2. Materials and Methods

2.1 Materials

2.1.1 Study site description

Turkey is a country between $26^0 - 45^0 E$ meridians and $36^0 - 42^0 N$ parallels as seen in Figure 1 (a) and it covers a 783.562 km^2 area. However, maximum and minimum estimation points are taken as 45^0 for the east, 25^0 for the west, 42.1^0 for the north and 36^0 for the south to in order to include all stations. For instance, the spatial location of Çanakkale Gökçeada station is between $25.91^0\ W$ and $40.19^0\ S$. Figure 1 (b) shows regions of Turkey.

2.1.2. Data description

In this study, the data between the years 2012 and 2016 have been utilized. Means and standard deviations of the data with Gaussian distribution were used as soft data. The data was taken from the web site of Turkey Ministry of Environment and Urban Planning for each station.

Both annual and seasonal estimations have been realized. In the annual estimation, 0.25^0, 0.5^0, 1^0 and 1.5^0 are used as spatial lags where ne week, two weeks and one month are taken as temporal lags. Zero and constant-local mean are chosen as kriging methods. Table 1 shows the study matrix for the annual prediction.

Map of stations are given in Figure 2 (a) and the data points after the kriging of BME approach is given in Figure 2 (b).

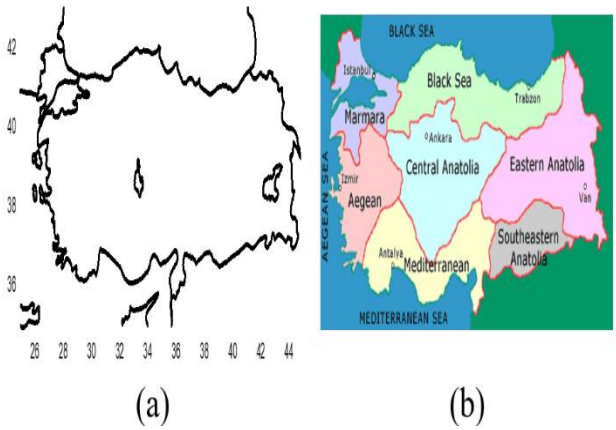

Figure 1. (a) Turkey latitude and longitude map (b) Turkey regions map

Table 1. Study matrix for the annual prediction

Spatial Lag	Temporal Lag	Local Mean
0.25^0 0.5^0 1^0 1.5^0	1 week 2 weeks 1 month	Zero (Simple kriging) Constant (Ordinary kriging)

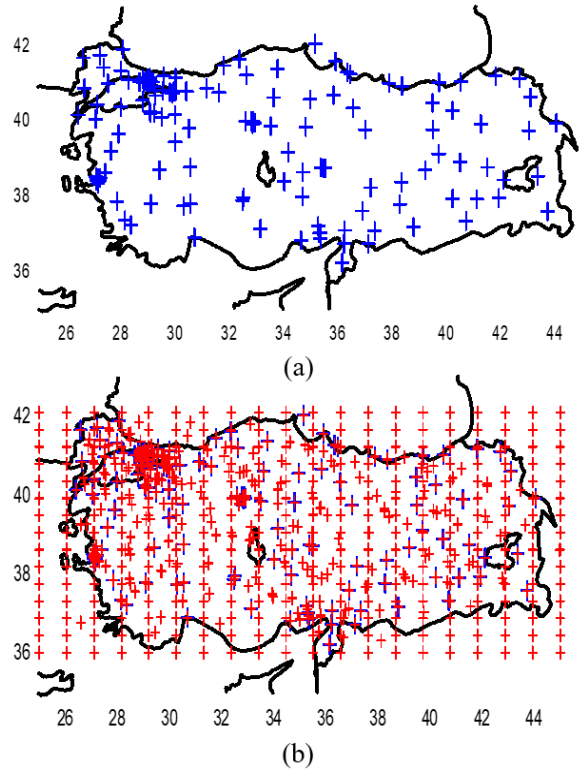

Figure 2. (a) The stations of the data (b) The data points after the kriging of BME approach

2.2 Method

2.2.1 The Bayesian Maximum Entropy (BME) Method

Space-time interpolation techniques do not consider secondary variables related to primary variables via empirical law while they explain raw data with cross-correlation between primary and secondary variables. However, empirical laws and soft data can be regarded for by BME [11]. This is a special property of BME.

Bayesian Maximum Entropy (BME) [1, 2, 3, 4, 5, 6] is a nonlinear geostatistical approach. It realizes spatiotemporal analysis and uses spatiotemporal domains. During processing of the data, physical rules, experiences, theories, high order space/time moments, outputs of models etc. are incorporated to the process.

In modern geostatistics, data sets χ_{data} consist of two basis categories as seen below [35].

$$S: \chi_{data} = (\chi_{hard}, \chi_{soft}) = (\chi_1, \dots, \chi_m) \quad (1)$$

where χ_{hard} and χ_{soft} show hard and soft data, respectively. In relation to hard data, specificatory knowledge for the points $m_h (< m)$ is

$$S: \chi_{hard} = (\chi_1, \dots, \chi_{m_h}) \quad (2)$$

Specificatory knowledge base (S) contains single-valued measurements $\chi_i (i = 1, \dots, m_h)$ in space/time. Regarding to the soft data, the specificatory knowledge for the remaining points $m_s = m - m_h$ is given as

$$S: \chi_{soft} = (\chi_{m_{h+1}}, \dots, \chi_m) \quad (3)$$

Figure 3 shows a framework of BME approach.

A spatiotemporal analysis begins with general knowledge base G. At the prior stage, the joint probability density function $f_G(\chi_{map})$ is calculated via general knowledge and maximum entropy theory is applied [36].

At the meta-prior stage, hard and soft data and specificatory knowledge base S are considered.

At the posterior stage, S and G are integrated to the mapping process [35].

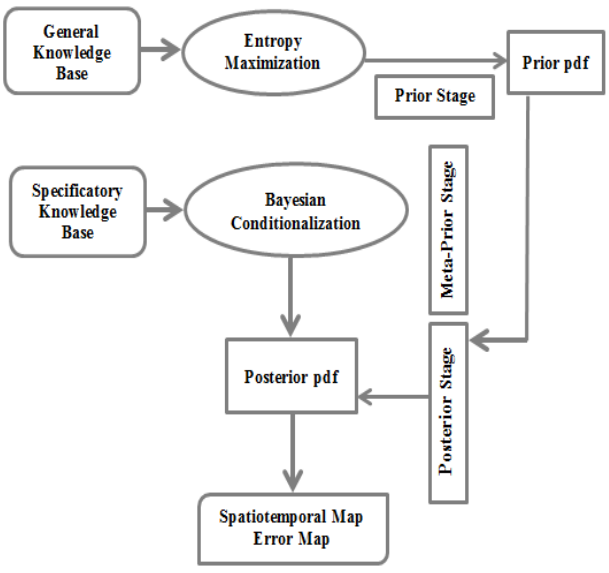

Figure 3. A conceptual framework of the BME approach.

BME posterior probability density function $f_k(\chi_k)$ is as follows [4, 35]

$$f_k(\chi_k) = A^{-1} \int d\chi_{soft} f_S(\chi_{soft})\, f_G(\chi_{hard}, \chi_{soft}, \chi_k) \quad (4)$$

where $\kappa = G \cup S$ is available all physical knowledge and A is a normalization parameter.

In this study, because it minimizes mean squared estimation errors, the conditional mean estimation is used.

As a rule, uncertainty measurements are given with variances of forecast errors [37, 38]. The variance of BME posterior pdf can be taken as a measure of a forecast error. Because this value is equivalent to the variance of a forecast error $e_k = x_k - \bar{x}_{k|\kappa}$, it is used as performance criteria.

For Gaussian posterior pdf, the probability of x_k which changes between the interval $[\bar{x}_{k|\kappa} - 1.96\sigma_{k|\kappa}, \bar{x}_{k|\kappa} + 1.96\sigma_{k|\kappa}]$ is 95% [7].

3. Results

Figure 4 a to f shows histograms and summary statistics for daily mean PM_{10} concentrations. From Figure 4(a) to 4(f), it is easily seen that daily mean PM_{10} concentrations are right-skewed series, namely; there is a density of low PM_{10} concentrations.

3.1. Annual prediction of PM_{10}

Regarding the study matrix, PM_{10} concentrations were predicted and the best results are obtained with a 1.5^0-spatial range and 1-week-temporal range and constant local mean. In Figure 5 (a) and (b), the mean PM_{10} concentrations and error variance map can be seen, respectively.

Figure 5. (a) Predicted mean PM_{10} values map (b) Error variance map.

From Figure 5 (a), the spatial variability can be seen. According to the national air quality index, the national limit value of PM_{10} for the year 2017 is 70 μg/m^3. Even though the mean PM_{10} concentration of Turkey is approximately 56 μ g/m^3, it is apparent that there are some regions which have PM_{10} concentrations that are beyond the national limit. Especially in the Southeastern Anatolia Region, high PM_{10} concentrations are prominent. The cities with high PM_{10} concentration are Aydın, Afyon, Zonguldak, Kastamonu, Sinop, Adana, Samsun, Ordu, Giresun, Şanlıurfa, Diyarbakır, Batman, Muş, Siirt, Ağrı, Kars, Hakkâri and Iğdır. Some former studies [39, 40, 16, 41] have remarked that usage of the fossil fuels for heating is relatively low in Southeastern Anatolia Region because winter temperatures in the region are not higher than Central and Eastern Anatolia Region. PM_{10} concentrations of the Southeastern Anatolia Region increase in spring, summer and autumn seasons due to desert dusts transported from North Africa, Arabia and Syria. Because this region is close to desert areas, on the transition path of mesoscale cyclones and located in Western winds zones due to its geographical location, desert dusts are the most important source of air pollution. Furthermore, the reason of high PM_{10} concentrations in the Black Sea Region may be explained with dry atmospheric conditions and thick inversion level near the ground surface of the Marmara Region as specified by Baltaci [41]. In addition, a thick dust layer transported from Libya and transportation of sea spray causes high PM_{10} concentrations in some cities in the Aegean Region [41, 42].

From Figure 5 (b), it can be said that error variance values of the areas which have higher PM_{10} concentrations are prominently low when compared to other areas with higher error variances. It is thought that, the reason of high error variance values may be due to the lack of air quality monitoring stations and/or available data in those areas.

3.2. Seasonal prediction of PM_{10}

Seasonal PM_{10} concentrations were predicted for all seasons, and best results were obtained with a 1^0-spatial range and 1-week-temporal range and for constant local mean for each of them. Figure 6 shows predicted mean PM_{10} concentration maps and error variance maps for spring, summer, autumn and winter seasons.

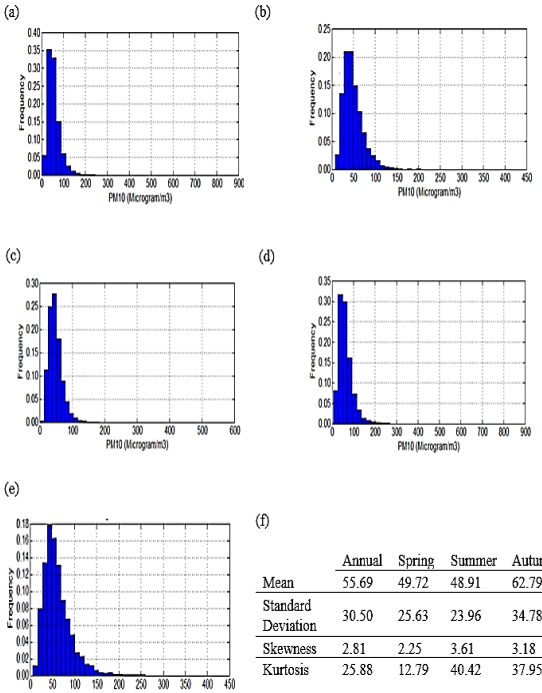

	Annual	Spring	Summer	Autumn	Winter
Mean	55.69	49.72	48.91	62.79	61.50
Standard Deviation	30.50	25.63	23.96	34.78	33.48
Skewness	2.81	2.25	3.61	3.18	2.07
Kurtosis	25.88	12.79	40.42	37.95	8.99

Figure 4. Histograms of daily mean PM_{10} concentrations (a) for all years (b) for spring seasons (c) for summer seasons (d) for autumn seasons (e) for winter seasons (f) Summary statistics

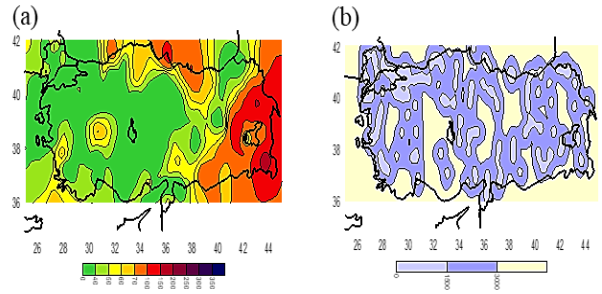

Figure 5. (a) Predicted mean PM_{10} values map (b) Error variance map

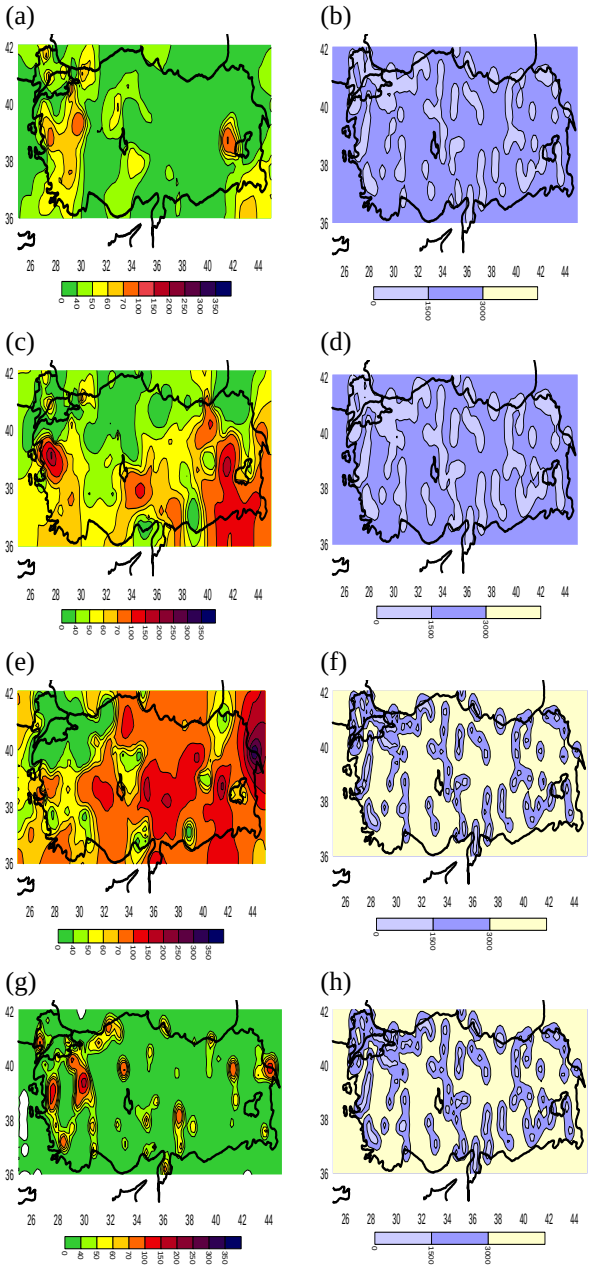

Figure 6. (a) Predicted mean PM_{10} values map for spring seasons (b) Error variance map for spring seasons (c) Predicted mean PM_{10} values map for summer seasons (d) Error variance map for summer seasons (e) Predicted mean PM_{10} values map for autumn seasons (f) Error variance map for autumn seasons (g) Predicted mean PM_{10} values map for winter seasons (h) Error variance map for winter seasons

For spring seasons, it can be said that average PM_{10} concentrations are between 24.1 $\mu g/m^3$ and 75.3 $\mu g/m^3$ as seen in the Figure 4 (f). The stations which have PM_{10} concentrations more than 70 $\mu g/m^3$ are Muş, Kütahya, Tekirdağ-Merkez, Bitlis, Yalova, Manisa, Denizli-Bayramyeri, Kırklareli, İstanbul-Aksaray, Kocaeli-Kandıra and Bursa. As seen from Figure 6 (a), Eastern and Central Black Sea Region are associated well with PM_{10} concentrations whereas there are high PM_{10} concentrations in Marmara, Aegean and Southeastern Regions. Besides, the cities which have the lowest-PM_{10} concentrations are Bingöl, Adana, Tunceli, Erzurum and Ardahan.

For summer seasons, it is determined from the Figure 4 (f) that average PM_{10} concentrationsare between 25 μ g/m^3 and 72.9 μ g/m^3. The stations with PM_{10} concentrations larger than 70 $\mu g/m^3$ are Manisa, Muş, Siirt, Niğde, Hakkâri, Bayburt, Kayseri-Hürriyet, Mardin, Ankara-Cebeci, Trabzon-Meydan, Balıkesir, İzmir, Tekirdağ, İstanbul, Denizli, Kocaeli, Karaman, Aksaray, Osmaniye, Kahramanmaraş, Gaziantep, Elazığ, Erzincan, Diyarbakır, Batman and Iğdır. In Figure 6 (c), it is clearly seen that there is a distinctive variability. While relatively high PM_{10} concentrations are appeared in the south and central part of the country, the north of the country has quite low PM_{10} concentrations. From this figure, it is concluded that nonconsumption of fossil fuels for residential heating is a decisive factor in summer seasons for most of the northern Turkey. Moreover, effects of desert dusts are explicit in the southeastern, eastern Anatolia and eastern Mediterranean Regions. In this season, the cities with the lowest-PM_{10} concentrations are Kocaeli, Şanlıurfa, Kırklareli, İstanbul and Kırıkkale.

For autumn seasons, it is seen in the Figure 4 (f), average PM_{10} concentrations change between 28 $\mu g/m^3$ and 97.6 μ g/m^3. The stations which have PM_{10} concentrations above 70 μ g/m^3 are Iğdır, Kayseri-Hürriyet, Muş, Erzincan, Kahramanmaraş-Elbistan, Osmaniye, Siirt, Hatay-Antakya, Batman, Kars-İstasyon Mahallesi, İzmir, Manisa, Afyon, Konya, Ankara, Karaman, Çankırı, Kastamonu, Niğde, Çorum, Amasya, Samsun, Tokat, Sivas, Gaziantep, Sivas, Ordu, Adıyaman, Malatya, Elazığ, Trabzon, Bayburt, Diyarbakır, Mardin, Ardahan, Ağrı, Hakkari and Van. Figure 6 (e) show that there are rather high PM_{10} concentrations are common in Turkey except Marmara Region. In this season, the cities with the lowest-PM_{10} concentrations are Çanakkale, İstanbul, Kocaeli, Yalova and Tekirdağ.

For winter seasons, average PM_{10} concentrations change between 28 $\mu g/m^3$ and 95 $\mu g/m^3$ as seen in the Figure 4 (f). The stations which have PM_{10} concentrations

above 70 μ g/m^3 are Kütahya, Iğdır, Ankara-Kayaş, Manisa-Soma, Bursa, Bursa-Beyazıt Caddesi, Erzurum, Edirne-Keşan, Bursa-Kestel, Muğla-Musluhittin, Edirne, İstanbul, Denizli, Uşak, Kocaeli, Iğdır, Eskişehir, Afyon, Isparta, Antalya, Düzce, Zonguldak, Karabük, Ankara, Niğde, Adana, Kayseri, Hatay, Kahramanmaraş, Gaziantep, Trabzon, Muş, Ağrı and Hakkâri. From Figure 6 (g), it can be concluded that desert dusts are the most important reason for large PM_{10} concentrations. Other than the abovementioned parts of Turkey, PM_{10} levels are low in winters. Furthermore, it can be said that the areas which have higher PM_{10} concentrations are generally industrial zones.

4. Conclusion

To decrease environmental pollution and public health risks, spatiotemporal mapping of air pollutants is necessary. From this point of view, the first and only spatiotemporal PM_{10} study including all regions of Turkey has been realized.

All variables like climatological conditions, agricultural activities, industries, residential heating types, topographical features, populations should be considered when interpreting PM_{10} levels. According to annual prediction results, Southeastern Anatolia Region has high PM_{10} concentrations. Closeness to deserts, western wind zones, being on the transition path of mesoscale cyclones can be regarded as reasons of high PM_{10} concentrations. Moreover, the eastern and middle part of the Black Sea Region, northeastern part of Central Anatolia, Aegean Region and eastern part of Turkey are high-PM_{10} zones.

According to seasonal PM_{10} maps, there are high PM_{10} concentrations especially in Summer and Autumn seasons. The highest PM_{10} concentrations are realized in Autumn seasons. Apart from major part of the Marmara Region, almost all regions have high PM_{10} concentrations in autumns. This situation can be explained by either the season is the desert dusts effective season or residential heating begins. Besides, the reason of relatively clear appearance of the Marmara Region may be due to wind effects. The PM_{10} prediction map of Summer seasons indicates high PM_{10} concentrations in the southwestern, eastern and northeastern part of Turkey and inner Aegean Region. The increase of PM_{10} in Autumn and Summer seasons may be associated from agricultural activities in addition to lack of rain and desert dusts. Also, these regions are less covered by forests pretending like natural dust filters than Black Sea Region as stated by Karaca [21].

Although Winter seasons have generally the most polluted air due to traffic-based emissions and residential heating, Turkey shows a different PM_{10} profile. Some regions of the Marmara, inner Aegean, Eastern and Central Anatolia Regions have high PM_{10} concentrations. The sources of this pollution may be industries, heating, traffic and climatic conditions. In addition, the Marmara, Aegean and Southeastern Regions have high PM_{10} concentrations in Spring seasons.

When viewed error variance maps, error variance values are higher in Autumn and Winter seasons than in Spring and Summer seasons since Autumn and Winter seasons have higher fluctuations and variability of PM_{10} concentrations and this situation may cause high error variance values.

One of the most important difficulties faced by the study is the lack of available data. The problems of missing or unreasonable data should be solved and the number of mobile stations should be increased.

For the future studies, it is aimed to realize multi-point mappings of PM_{10} and generating other air pollutants' maps. Furthermore, epidemiologic studies which are focusing on the relationship between PM_{10} values and some diseases especially respiratory disorders should be analyzed and mapped.

Declaration

The author(s) declared no potential conflicts of interest with respect to the research, authorship, and/or publication of this article. The author(s) also declared that this article is original, was prepared in accordance with international publication and research ethics, and ethical committee permission or any special permission is not required.

References

1. Christakos, G. A *Bayesian maximum-entropy view to the spatial estimation problem*. Mathematical Geology, 1990. **22**(7), 763-777.
2. Christakos, G. *Some applications of the Bayesian, maximum entropy concept in Geostatistics*. Fundamental Theories of Physics, 1991a. p.215-229. Kluwer Acad. Publ. Dordrecht, The Netherlands.
3. Christakos, G. *A theory of spatiotemporal random fields and its application to space-time data processing*. IEEE Trans., Systems, Man & Cybernetics, 1991b. V. 21, No.4, p. 861-875.
4. Christakos, G. *Random Field Models in Earth Sciences*. 1992, Academic Press, San Diego, CA.
5. Christakos, G. *Spatiotemporal information systems in soil and environmental sciences*. Geoderma, 1998a. **85**(2), 141-179.
6. Christakos, G. *Multi-point BME space/time mapping of environmental variables.* Computational Methods in Water Resources XII 1998b, Computational Methods in Surface and Groundwater Transport. Computational Mechanics Publ., 1998b. Vol.2., p. 289-296, Southampton, UK.
7. Serre M.L. and Christakos, G. *Modern Geostatistics: Computational BME analysis in the light of uncertain physical knowledge-the Equus Beds study*. Stochastic

Environmental Research and Risk Assessment, 1999. **13**(1-2), p.1-26.

8. Serre M.L., Kolovos, A., Christakos, G., and Modis, K. *An application of the holistochastic human exposure methodology to naturally occuring arsenic in bangladesh drinking water*. Risk Analysis, 2003. **23**(3), p.525-528.
9. Bogaert, P., Christakos, G., Jerrett, M., and Yu, H.L. *Spatiotemporal modelling of ozone distribution in the State of California*. Atmospheric Environment, 2009. **43**(15), p.2471-2480.
10. Fan, L., Xiao, Q., Wen, J., Liu, Q., Jin, R., You, D., and Li, X. *Mapping high-resolution soil moisture over heterogeneous cropland using multi-resource remote sensing and ground observations*. Remote Sensing, 2015. **7**, p.13273-13297.
11. Shi, T., Yang, X., Christakos, G., Wang, J. and Li, L. *Spatiotemporal interpolation of rainfall by combining bme theory and satellite rainfall estimates*. Atmosphere, 2015. **6**(9), p.1307-1326.
12. Douaik, A., Van Meirvenne, M., Toth, T., and Serre, M. *Space-time mapping of soil salinity using probabilistic bayesian maximum entropy.* Stoch. Envir. Res. And Risk Ass., 2004. **18**, p.219-227.
13. Tang, S., Yang, X., Dong, D., and Li, Z. *Merging daily sea surface temperature data from multiple satellites using a Bayesian maximum entropy method.* Front. Earth Sci., 2015. **9**(4): p.722-731.
14. Baydaroğlu, Ö., and Koçak, K. *Spatiotemporal analysis of wind speed via the Bayesian Maximum Entropy*. Environmental Earth Sciences, 2019. **78**(1), 17.
15. Alyuz, U., Alp, K. *Emission inventory of primary air pollutants in 2010 from industrial processes in Turkey*. Science of the Total Environment, 2014. **488**, p.369-381.
16. Kabatas, B., Unal, A., Pierce, R.B., Kindap, T., and Pozzoli, L. *The contribution of Saharan dust in PM_{10} concentration levels in Anatolian Peninsula of Turkey*. Science of the Total Environment, 2014. **488**, p.413-421.
17. Güler, N., and İşçi, Ö.G. *The regional prediction model of PM_{10} concentrations for Turkey*. Atmospheric Research, 2016. **180**, p.64-77.
18. Ozel, G., and Cakmakyapan, S. *A new approach to the prediction of PM_{10} concentrations in Central Anatolia Region, Turkey*. Atmospheric Pollution Research, 2015. **6**(5), p.735-741.
19. Im, U., Markakis, K., Unal, A., Kindap, T., Poupkou, A., Incecik, S., ..., and Mihalopoulos, N. *Study of a winter PM episode in Istanbul using the high resolution WRF/CMAQ modeling system*. Atmospheric Environment, 2010. **44**(26), p.3085-3094.
20. Şahin, Ü.A., Ucan, O.N., Bayat, C., and Tolluoglu, O. *A new approach to prediction of SO2 and PM_{10} concentrations in Istanbul, Turkey: Cellular Neural Network (CNN).* Environmental Forensics, 2011. **12**(3), p.253-269.
21. Karaca, F. *Determination of air quality zones in Turkey.* Journal of the Air & Waste Management Association, 2012. **62**(4), p.408-419.
22. Konovalov, I.B., Beekmann, M., Meleux, F., Dutot, A, and Foret, G. *Combining deterministic and statistical approaches for PM_{10} forecasting in Europe*. Atmospheric Environment, 2009. **43**(40), p.6425-6434.
23. Nonnemacher, M., Jakobs, H., Viehmann, A., Vanberg, I., Kessler, C., Moebus, S., ..., and Heinz Nixdorf Recall Study Investigative Group. *Spatio-temporal modelling of residential exposure to particulate matter and gaseous pollutants for the Heinz Nixdorf Recall Cohort*. Atmospheric Environment, 2014. **91**, p.15-23.
24. Djalalova, I., Wilczak, J., McKeen, S., Grell, G., Peckham, S., Pagowski, M., ..., and McHenry, J. *Ensemble and bias-correction techniques for air quality model forecasts of surface O3 and PM 2.5 during the TEXAQS-II experiment of 2006*. Atmospheric Environment, 2010. **44**(4), p.455-467.
25. Debry, E., and Mallet, V. *Ensemble forecasting with machine learning algorithms for ozone, nitrogen dioxide and PM_{10} on the Prev'Air platform*. Atmospheric Environment, 2014. **91**, p.71-84.
26. Chen, Y., Shi, R., Shu, S., and Gao, W. *Ensemble and enhanced PM_{10} concentration forecast model based on stepwise regression and wavelet analysis.* Atmospheric Environment, 2013. **74**, p.346-359.
27. Kim, S.Y., and Song, I. *National-scale exposure prediction for long-term concentrations of particulate matter and nitrogen dioxide in South Korea*. Environmental Pollution, 2017. **226**, p.21-29.
28. Christakos, G. and Serre, M.L. *BME analysis of spatiotemporal particulate matter distributions in North Carolina.* Atmospheric Environment, 2000. **34**(20), p.3393-3406.
29. Puangthongthub, S., Wangwongwatana, S., Kamens, R.M., and Serre, M.L. *Modeling the space/time distribution of particulate matter in Thailand and optimizing its monitoring network.* Atmospheric Environment, 2007. **41**(36), p.7788-7805.
30. Yu, H.L., Chen, J.C., Christakos, G., and Jerrett, M. *BME Estimation of Residential Exposure to Ambient PM_{10} and Ozone at Multiple Time Scales*. Environmental Health Perspectives, 2009. **117**(4), 537.
31. Fernando, H.J., Mammarella, M.C., Grandoni, G., Fedele, P., Di Marco, R., Dimitrova, R., and Hyde, P. *Forecasting PM 10 in metropolitan areas: efficacy of neural networks.* Environmental Pollution, 2012. **163**, p.62-67.
32. Akita, Y., Chen, J.C., and Serre, M.L. *The moving-window Bayesian maximum entropy framework: estimation of PM2. 5 yearly average concentration across the contiguous United States*. Journal of Exposure Science and Environmental Epidemiology, 2012. **22**(5), p.496-501.
33. Beckerman, B.S., Jerrett, M., Serre, M., Martin, R.V., Lee, S.J., Van Donkelaar, A., ..., and Burnett, R.T. *A hybrid approach to estimating national scale spatiotemporal variability of $PM_{2.5}$ in the contiguous United States*. Environmental Science & Technology, 2013. **47**(13), 7233.
34. Bayesian Maximum Entropy Graphical Users Interface (BMEGUI), University of North Carolina. [cited 2015 May 1]. Available from: http://www.unc.edu/depts/case/BMEGUI/BMEGUI3.0.1/BMEGUI3.0.1_WEB_2014. htm
35. Christakos, G. *Modern Spatiotemporal Geostatistics*, 2000. Oxford University Press.
36. Gao, S., Zhu, Z., Liu, S., Jin, R., Yang, G., and Tan, L. *Estimating the spatial distribution of soil moisture based on Bayesian maximum entropy method with auxiliary data from remote sensing.* International Journal of Applied Earth Observation and Geoinformation, 2014. **32**, p.54-66.

37. Olea, R.A. *Understanding Geostatistics*. Course Notes, 1997. Civil Engineering Dept., Univ. of Kansas, Lawrence, KS.
38. Bogaert, P., and Christakos, G. *Spatiotemporal analysis and processing of thermometric data over* Belgium. Journal of Geophysical Research-All Series-, 1997. **102**, p.25-831.
39. Şengün, T. and Kıranşan, K. *Güneydoğu Anadolu Bölgesi'nde çöl tozlarının hava kalitesi üzerine etkisi.* Türk Coğrafya Dergisi, 2012. (**59**) (in Turkish).
40. Dolar, A. and Saraç, H.T.K. *Türkiye'nin doğu illerindeki hava Kalitesinin PM_{10} açısından incelenmesi* (In Turkish) Iğdır Univ. J. Inst. Sci. & Tech., 2015. **5**(4): p.25-32.
41. Baltaci, H. *Spatial and Temporal Variation of the Extreme Saharan Dust Event over Turkey in March 2016*. Atmosphere, 2017. **8**(2), 41.
42. Koçak, M., Mihalopoulos, N., and Kubilay, N. *Contributions of natural sources to high PM10 and PM2.5 events in the eastern Mediterranean*. Atmospheric Environment, 2007. **41**(18), p. 3806-3818.